

**RATIONALIZATION IN DERIVING ELEMENT STIFFNESS MATRIX  
BY ASSUMED STRESS APPROACH**

Theodore H. H. Pian\*\* and Pin Tong\*\*\*  
Massachusetts Institute of Technology

From the principle of minimum complementary energy which is extended to take into account the possible discontinuity in stresses or displacements along the interelement boundaries, the finite element methods by both the assumed stress hybrid model and the equilibrium model can be formulated. This formulation enables the development of a rational method for consistent lumping of body and surface forces and the establishment of a criterion for the kinematical instability of a system. For the hybrid model, there is an optimum choice of the number of stress modes for a given boundary displacement approximation. Example calculations for plate-bending problems are included to substantiate the analytical predictions. Examples are also carried out to illustrate the convenience in taking transverse shear effects into account by the hybrid method.

---

\*Work described in this paper was sponsored in whole by the Air Force Office of Scientific Research under Contract F44620-67-C-0019.

\*\*Professor of Aeronautics and Astronautics

\*\*\*Assistant Professor of Aeronautics and Astronautics

SECTION I  
INTRODUCTION

When the assumed stress hybrid model was suggested by Pian (References 1 and 2) to derive the element stiffness matrices, the complementary energy of only the individual elements was considered. Later on, a variational principle was developed (Reference 3) to treat the entire assembled elements as a whole. It was then possible to derive the loading matrix in a consistent manner and to reveal some restrictions in the formulation of the assumed stress hybrid method.

The present paper is to derive a variational principle which can, in fact, cover both the assumed stress hybrid model and the equilibrium model by Fraeijs de Veubeke (Reference 4 and 5); hence some of the characteristics are common to both methods. The formulation of the hybrid model is then extended to plate-bending problems including both thermal effect and transverse shear effect. Example calculations are made to evaluate this method.

SECTION II

PRINCIPLE OF MINIMUM COMPLEMENTARY ENERGY-  
EQUILIBRIUM MODEL AND ASSUMED STRESS HYBRID MODEL

Both the equilibrium model and the assumed stress hybrid model for finite element analysis can be derived from the principle of minimum complementary energy, for which the functional to be varied is

$$\pi_c = \int_V \frac{1}{2} C_{ijkl} \sigma_{ij} \sigma_{kl} \, dV - \int_{S_u} T_i \bar{u}_i \, dS \quad (1)$$

In this expression

- $\sigma_{ij}$  = stress tensor
- $C_{ijkl}$  = elastic compliance tensor
- $V$  = volume
- $S$  = surface
- $T_i$  = surface traction
- $\bar{u}_i$  = prescribed boundary displacement
- $S_u$  = portion of  $S$  over which the boundary displacements  $u_i$  are prescribed

The stress tensor  $\sigma_{ij}$  satisfies the equilibrium conditions

$$\sigma_{ij,j} + \bar{F}_i = 0 \quad (2)$$

and is compatible with the prescribed boundary tractions over the boundary  $S_\sigma$ .  $\bar{F}_i$  is the prescribed body force.

In applying the finite element method, the assumed stress field need not be continuous across the interelement boundaries, but equilibrium must be maintained for the surface tractions  $T_i$ , defined by  $T_i = \sigma_{ij} \nu_j$ , where  $\nu_j$  are the components of the unit vector normal to the boundary. Let two neighboring elements "a" and "b" be isolated (Figure 1), and consider the boundary traction components  $T_i^{(a)}(s)$  and  $T_i^{(b)}(s)$  ( $i = 1,2,3$ ) over the respective sides of the common boundary AB. (For simplicity, a plane stress example is used for illustration.)

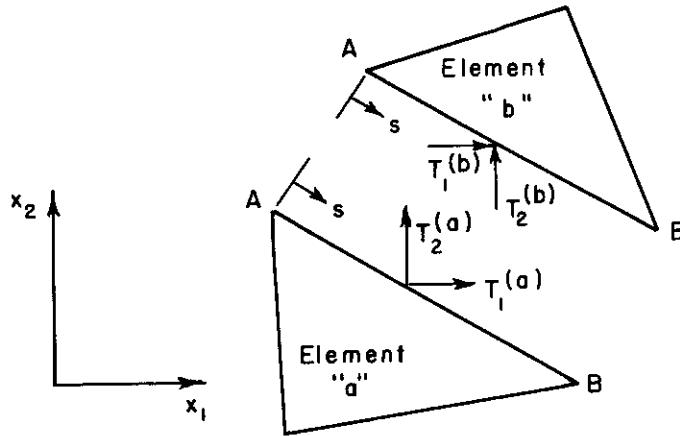


Figure 1. Equilibrium of Boundary Traction Along Interelement Boundary

The equilibrium conditions at the interelement boundary are given by

$$T_i^{(a)}(s) + T_i^{(b)}(s) = 0 \quad (i = 1, 2, 3) \quad (3)$$

Equation 3 may be considered as conditions of constraint and can be introduced by including Lagrange multiplier terms

$$\int_{AB} \lambda_i(s) [T_i^{(a)}(s) + T_i^{(b)}(s)] ds \quad (4)$$

or

$$\int_{AB} \lambda_i T_i ds \Big|_{"a"} + \int_{AB} \lambda_i T_i ds \Big|_{"b"}$$

in the complementary energy functional to be varied. The Lagrange multipliers  $\lambda_i$ , which are functions of the surface coordinates, are to be treated as additional variables.

When all the interelement boundaries have been considered, the complementary energy functional may be written as:

$$\begin{aligned} \pi = \sum_n \left( \int_{V_n} \frac{1}{2} C_{ijkl} \sigma_{ij} \sigma_{kl} dV \right. \\ \left. - \int_{S_n} \lambda_i T_i dS - \int_{S_{u_n}} T_i \bar{u}_i dS \right) \quad (5) \end{aligned}$$

where  $S_{u_n}$  is the boundary of  $V_n$  where the displacements are prescribed and  $S_n$  is the interelement boundary of  $V_n$ . By taking the variation of  $\pi$  with respect to  $\sigma_{ij}$  and  $\lambda_i$ , it is easily shown that the Lagrange multipliers  $\lambda_i$  are equal to  $u_i$ , the displacements along the interelement boundary

$$\pi = \sum_n \left( \int_{V_n} \frac{1}{2} c_{ijkl} \sigma_{ij} \sigma_{kl} dV - \int_{S_n} T_i u_i dS - \int_{S_{u_n}} T_i \bar{u}_i dS \right) \quad (6)$$

In the finite element solution, the assumed approximate functions for the stresses  $\sigma_{ij}$  are divided into two parts. The first part, which consists of a finite number of parameters  $\beta$ , should satisfy the homogeneous equations of equilibrium, while the second part is a particular solution of the equations of equilibrium with the prescribed body forces. In matrix form, the stresses  $\sigma_{ij}$  are expressed as:

$$\sigma = P \beta + P_F \beta_F \quad (7)$$

where  $\beta$  is unknown and  $P_F \beta_F$  is determined from the particular solution. For elements which contain boundaries with prescribed surface tractions, some of the  $\beta$ 's in the first term will also be prescribed. In this case, all the prescribed  $\beta$ 's are put in the second term.

Both the equilibrium and the hybrid methods can be derived from Equation 6, but the distinction lies in the treatment of the surface integrals along the interelement boundaries. For the equilibrium model, the surface tractions  $T_i$  along each boundary are represented uniquely by the generalized loads  $Q$  pertaining to the boundary and can be written as

$$T = \phi Q \quad (8)$$

For example, when  $Q$  are the values of  $T_i$  at a finite number of boundary points,  $\phi$  represents the corresponding interpolation functions. Since the surface tractions are also related to the assumed stress distribution, they can also be expressed as

$$T = R \beta + R_F \beta_F \quad (9)$$

Thus, there is a unique relation between  $Q$  and  $\beta$  of the form:

$$Q = G^T \beta + G_F^T \beta_F \quad (10)$$

The corresponding element generalized displacements  $q$  are defined by:

$$Q^T q = \int_{S_n} T_i u_i dS = Q^T \int_{S_n} \phi^T u_B dS \quad (11)$$

or

$$\mathbf{q} = \int_{S_n} \phi^T \mathbf{u}_B \, dS \quad (12)$$

Thus, the generalized displacement is a weighted integral of the boundary displacements, and to maintain the same  $\mathbf{q}$  for two neighboring elements does not guarantee compatibility along the entire boundary. It is seen that, in an equilibrium model, each generalized displacement is common to only two neighboring elements.

For the hybrid method, the approximate displacements along the interelement boundaries are represented by interpolation functions and the generalized displacements  $\mathbf{q}$  at a finite number of boundary nodes:

$$\mathbf{u}_B = \mathbf{L} \mathbf{q} \quad (13)$$

Since the interpolating functions  $\mathbf{L}$  are applied to the individual boundary segments, they are relatively easy to construct so that interelement compatibility is maintained. Unlike the equilibrium model, the generalized displacements  $\mathbf{q}$  may be referred to corner nodes where more than two elements are connected.

The corresponding generalized nodal forces are defined again by:

$$\mathbf{q}^T \mathbf{Q} = \int_{S_n} T_i u_i \, dS \quad (14)$$

or

$$\mathbf{Q} = \int_{S_n} \mathbf{L}^T \mathbf{T} \, dS \quad (15)$$

Thus, the generalized nodal force is a weighted integral of the boundary tractions, and to maintain equilibrium at a node does not guarantee equilibrium over the entire boundary. Another significant difference from the equilibrium model is that the stresses and the boundary displacements are independently assumed. Hence, the number of parameters in  $\beta$  and the number of generalized displacements  $\mathbf{q}$  can be chosen independently in the hybrid model.

Finally, since the hybrid method relies on assumed boundary displacements, the prescribed boundary stresses no longer constitute a restrained boundary condition. In this case the functional  $\pi$  can be written more conveniently as

$$\begin{aligned} \pi = \sum_n \left( \int_{V_n} \frac{1}{2} c_{ijkl} \sigma_{ij} \sigma_{kl} \, dV \right. \\ \left. - \int_{\partial V_n} T_i u_i \, dS + \int_{S_n} \bar{T}_i u_i \, dS \right) \quad (16) \end{aligned}$$

where

$$\partial V_n = S_n + S_{\sigma_n} + S_{u_n}$$

is the entire boundary of  $V_n$ , and  $u_i = \bar{u}_i$  on  $S_{u_n}$ .

Substitution of Equations 7, 10, and 11 into Equation 6 and substitution of Equations 7, 9, and 13 into Equation 16 both yield equations of the form

$$\begin{aligned} \pi = \sum_n \left( \frac{1}{2} \beta^T H \beta + \beta^T H_F \beta_F - \beta^T G q \right. \\ \left. + s^T q + B_n \right) \end{aligned} \quad (17)$$

where

$$\begin{aligned} H &= \int_{V_n} P^T C P \, dV \\ H_F &= \int_{V_n} P^T C P_F \, dV \\ B_n &= \frac{1}{2} \beta_F^T \int_{V_n} P_F^T C P_F \, dV \beta_F \end{aligned} \quad (18)$$

and  $C$  is the elastic compliance matrix. For the equilibrium model,  $G$  and  $G_F$  are defined by Equation 10. For the hybrid model they are given by:

$$G = \int_{\partial V_n} R^T L \, dS ; \quad G_F = \int_{\partial V_n} R_F^T L \, dS \quad (19)$$

The vector  $s^T$  is also different for the two models

$$\begin{aligned} s^T &= -\beta_F G_F \quad (\text{equilibrium model}) \\ s^T &= -\beta_F G_F + \int_{S_{\sigma_n}} \bar{T}^T L \, dS \quad (\text{hybrid model}) \end{aligned} \quad (20)$$

where  $\bar{T}$  are the prescribed boundary tractions.

The stationary conditions of the functional given by Equation 17 with respect to variations of  $\beta$  and  $q$  then yield

$$H \beta + H_F \beta_F - G q = 0 \quad (21)$$

and

$$\sum_n (\beta^T G - s^T) \delta q = 0 \quad (22)$$

By solving for  $\beta$  from Equation 21 and substituting back into Equation 17, we can express the functional  $\pi$  in terms of the generalized displacements  $q$  only, i.e.,

$$\pi = - \sum_n \left( \frac{1}{2} q^T k q - \bar{Q}^T q + c_n \right) \quad (23)$$

where  $k$  and  $\bar{Q}$  are, respectively, the element stiffness matrix and equivalent nodal forces defined by

$$k = G^T H^{-1} G \quad (24)$$

$$\bar{Q} = G^T H^{-1} H_F \beta_F + s \quad (25)$$

and

$$c_n = \frac{1}{2} \beta_F^T H_F^T H^{-1} H_F \beta_F - B_n = \text{Constant} \quad (26)$$

Knowing  $k$  and  $\bar{Q}$  for all elements, it is then a routine matter to set up the assembled matrix equation for the problem.

Inspection of Equation 22 reveals that if  $N$ , the total number of assumed stress modes  $\beta$  of all elements is smaller than  $M$ , the total number of unknown displacements  $q$ , there will be, in general, no solution for the  $\beta$ 's. It can be seen that the above situation corresponds to the appearance of kinematical deformation modes discussed by Fraeijs de Veubeke (Reference 5), who indeed had pointed out that for a single element, if  $n$  is the total number of stress modes and  $m$ , the number of generalized displacements of which  $r$  must be constrained,  $r$  being the rigid body degrees of freedom, then for such element to be kinematically stable,  $n$  must be larger than  $(m - r)$ . It is obvious that such requirements on the minimum number of stress modes can always be met by the hybrid model because the stress modes and boundary displacements are assumed independently, but it is not so for the equilibrium model. Furthermore, since for the hybrid model, there will always be more than two elements meeting at an internal node, the assembled structure will be kinematically stable if the above criterion for each individual element is satisfied. For the equilibrium model, however, an assembled structure may be unstable even if all the individual elements satisfy the criterion for kinematical stability (Reference 5).



SECTION III  
 COMPLEMENTARY ENERGY PRINCIPLE FOR PLATE THEORY  
 INCLUDING THERMAL AND TRANSVERSE SHEAR EFFECTS

The thermal effect is usually included in the variational principle as an initial strain problem (Reference 6). Let  $\epsilon_{oij}$  be the initial strain and  $\epsilon_{ij}$  the strain due to total deformation, then the stress is given by

$$\sigma_{ij} = E_{ijkl} (\epsilon_{kl} - \epsilon_{okl}) \quad (27)$$

It is convenient to define

$$\begin{aligned} \sigma'_{ij} &= E_{ijkl} \epsilon_{kl} = \text{stress associated with the total deformation} \\ \sigma_{oij} &= E_{ijkl} \epsilon_{okl} = \text{stress associated with the initial strain} \end{aligned} \quad (28)$$

Then

$$\sigma_{ij} = \sigma'_{ij} - \sigma_{oij} \quad (29)$$

For the plate-bending problem, it is more convenient to use  $\sigma'_{\alpha\beta}$  as the primary variable because the in-plane stress  $\sigma'_{\alpha\beta}$  varies linearly across the thickness; hence can be defined uniquely by the stress resultants  $N'_{\alpha\beta}$  and stress couples  $M'_{\alpha\beta}$ , i.e.,

$$\sigma'_{\alpha\beta} = \frac{N'_{\alpha\beta}}{h} + \frac{12M'_{\alpha\beta} x_3}{h^3} \quad (30)$$

Here the Greek index takes the value of 1 and 2 and the coordinate normal to the mid-plane is  $x_3$ . (Figure 2)

For the plate theory including transverse shear effect, the development in the following is based on the treatment of Reissner (Reference 7).

Substituting Equations 29 and 30 into the equilibrium equations in three-dimensional elasticity

$$\sigma_{ij,j} = 0 \quad (31)$$

for  $i = 1,2$  and integrating through the thickness direction we obtain the expressions for the transverse shear stress which satisfy the shear free conditions on both faces of the plate is

$$\sigma_{\alpha 3} = \frac{3Q'_{\alpha}}{2h} \left[ 1 - \left( \frac{2x_3}{h} \right)^2 \right] - \theta_{\alpha} \quad (32)$$

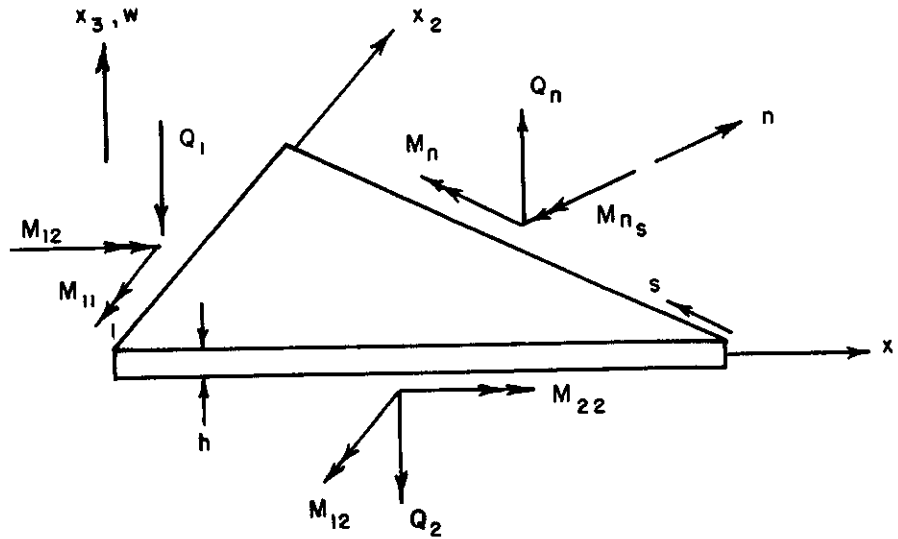


Figure 2. Sign Convention for Plate-Bending Problem

where

$$B_{\alpha} = \left( \frac{x_3}{h} + \frac{1}{2} \right) \int_{-h/2}^{h/2} \sigma_{\alpha\beta, \beta} dx_3 - \int_{-h/2}^{x_3} \sigma_{\alpha\beta, \beta} dx_3 \quad (33)$$

$$Q'_{\alpha} = M'_{\alpha\beta, \beta} = \text{transverse shear} \quad (34)$$

The substitution of Equation 32 into Equation 31 for  $i = 3$ , and integration along  $x_3$ , yields

$$\sigma_{33} = -\frac{3}{4} Q'_{\alpha, \alpha} \left[ \frac{2}{3} + \frac{2x_3}{h} - \frac{1}{3} \left( \frac{2x_3}{h} \right)^3 \right] + \int_{-h/2}^{x_3} B_{\alpha, \alpha} dx_3 \quad (35)$$

with  $\sigma_{33}(-h/2) = 0$ . By introducing the condition  $\sigma_{33}(+h/2) = p$ , we obtain

$$Q'_{\alpha, \alpha} = -p + \int_{-h/2}^{h/2} B_{\alpha, \alpha} dx_3 \quad (36)$$

It is obvious that the terms involve  $B_{\alpha}$  in Equation 32 and  $B_{\alpha\alpha}$  in Equations 35 and 36 are the stresses due to thermal effect in the present plate theory

$$\begin{aligned} \sigma_{\alpha\alpha_3} &= B_{\alpha} \\ \sigma_{\alpha_3\alpha} &= \frac{3}{4} \left[ \frac{2}{3} + \frac{2x_3}{h} - \left( \frac{2x_3}{h} \right)^3 \right] \int_{-h/2}^{h/2} B_{\alpha, \alpha} dx_3 - \int_{-h/2}^{x_3} B_{\alpha, \alpha} dx_3 \end{aligned} \quad (37)$$

The complementary energy functional can be expressed in terms of either  $\sigma_{ij}$  or  $\sigma'_{ij}$ , i.e.,

$$\pi_c = \int_{-h/2}^{h/2} \int_A \left( \frac{1}{2} C_{ijkl} \sigma_{ij} \sigma_{kl} + \epsilon_{oij} \sigma_{ij} \right) dA dx_3 - \int_{-h/2}^{h/2} \int_{s_u} \sigma_{ij} \nu_j \bar{u}_i ds dx_3 \quad (38)$$

or

$$\pi_c = \int_{-h/2}^{h/2} \int_A \frac{1}{2} C_{ijkl} \sigma'_{ij} \sigma'_{kl} dA dx_3 - \int_{-h/2}^{h/2} \int_{s_u} \sigma'_{ij} \nu_j \bar{u}_i ds dx_3 \quad (39)$$

By limiting our discussion to bending problems only and by expressing the stress due to deformation in the same form as that of Reference 7

$$\begin{aligned} \sigma'_{\alpha\beta} &= \frac{12 M'_{\alpha\beta} x_3}{h^3} \\ \sigma'_{\alpha 3} &= \frac{3Q'_{\alpha}}{2h} \left[ 1 - \left( \frac{2x_3}{h} \right)^2 \right] \\ \sigma'_{33} &= \frac{3}{4} p \left[ \frac{2}{3} + \frac{2x_3}{h} - \left( \frac{2x_3}{h} \right)^3 \right] \end{aligned} \quad (40)$$

Substituting into Equation 39 and carrying out the integration with respect to  $x_3$  we obtain the complementary energy functional in terms of  $M'_{\alpha\beta}$  and  $Q'_{\alpha}$ .

$$\begin{aligned} \pi_c &= \frac{1}{2} \int_A \frac{12}{h^3} \left[ C_{\alpha\beta\lambda\theta} M'_{\alpha\beta} M'_{\lambda\theta} + \frac{2}{5} h^2 C_{\alpha 3\beta 3} Q'_{\alpha} Q'_{\beta} \right. \\ &\quad \left. + \frac{h^2}{5} C_{\alpha\beta 33} M'_{\alpha\beta} p + \frac{h^3}{6} C_{\alpha 333} Q'_{\alpha} p \right] dA \\ &\quad - \int_{s_u} \left[ M'_{\alpha\beta} \nu_{\beta} \bar{\phi}_{\alpha} - Q'_{\alpha} \nu_{\alpha} \bar{w} \right] ds \end{aligned} \quad (41)$$

where  $\phi_{\alpha}$  is the rotations such that

$$u_{\alpha} = x_3 \phi_{\alpha}$$

and  $w$  is the normal displacement of the plate.

We can also express the complementary energy functional in terms of  $M_{\alpha\beta}$  and  $Q_{\alpha}$ . By defining the stress couples and transverse shears as

$$M_{\alpha\beta} = \int_{-h/2}^{h/2} x_3 \sigma_{\alpha\beta} dx_3 ; \quad Q_{\alpha} = \int_{-h/2}^{h/2} \sigma_{\alpha 3} dx_3 \quad (42)$$

and by writing

$$\begin{aligned} M_{\alpha\beta} &= M'_{\alpha\beta} - M_{0\alpha\beta} \\ Q_{\alpha} &= Q'_{\alpha} - Q_{0\alpha} \end{aligned} \quad (43)$$

we can easily identify that

$$M_{0\alpha\beta} = \int_{-h/2}^{h/2} x_3 \sigma_{0\alpha\beta} dx_3 \quad (44)$$

and

$$Q_{0\alpha} = \int_{-h/2}^{h/2} \sigma_{0\alpha 3} dx_3$$

and that  $Q_{\alpha}$  and  $M_{\alpha\beta}$  satisfy the conventional plate equilibrium equations. In terms of  $M_{\alpha\beta}$  and  $Q_{\alpha}$ , the functional  $\pi_c$  is

$$\begin{aligned} \pi_c &= \frac{1}{2} \int_A \frac{12}{h^3} \left[ C_{\alpha\beta\lambda\theta} M_{\alpha\beta} M_{\lambda\theta} + \frac{2}{5} h^2 C_{\alpha 3\beta 3} Q_{\alpha} Q_{\beta} \right. \\ &\quad \left. + \frac{h^2}{5} C_{\alpha\beta 33} M_{\alpha\beta} \rho + \frac{h^3}{6} C_{\alpha 3\beta 3} Q_{\alpha} \rho \right] dA \\ &\quad - \frac{1}{2} \int_A \frac{12}{h^3} \left[ 2C_{\alpha\beta\lambda\theta} M_{\alpha\beta} M_{0\lambda\theta} + \frac{4h^2}{5} C_{\alpha 3\beta 3} Q_{\alpha} Q_{0\beta} \right] dA \\ &\quad - \int_{s_u} (M_{\alpha\beta} \nu_{\beta} \bar{\phi}_{\alpha} - Q_{\alpha} \nu_{\alpha} \bar{w}) ds \end{aligned} \quad (45)$$

In the following special cases, the expressions for the complementary energy can be simplified. For example:

1. Isotropic material with thermal strain

$$\begin{aligned} \pi_c &= \frac{1}{2} \int_A \frac{12}{Eh^3} \left[ (M_x + M_y)^2 + 2(1+\nu)(M_{xy}^2 - M_x M_y) \right. \\ &\quad \left. + \frac{1+\nu}{5} h^2 (Q_x^2 + Q_y^2) - \frac{h^2}{5} \nu \rho (M_x + M_y) \right] dA \\ &\quad - \int_A \frac{12}{Eh^3} (1-\nu) M_0 (M_x + M_y) dA \\ &\quad - \int_{s_u} (M_n \bar{\phi}_n + M_{ns} \bar{\phi}_s - Q_n \bar{w}) ds \end{aligned} \quad (46)$$

where

$$M_o = \int_{-h/2}^{h/2} \frac{z E \alpha \Delta T (1-2\nu)}{1-\nu^2} dz \quad (47)$$

2. Conventional plate theory with thermal strain but with transverse shear effect

$$\begin{aligned} \pi_c = & \frac{1}{2} \int_A \frac{12}{Eh^3} \left[ (M_x + M_y)^2 + 2(1+\nu)(M_{xy}^2 - M_x M_y) \right] dA \\ & - \int_A \frac{12}{Eh^3} (1-\nu) M_o (M_x + M_y) dA \\ & - \int_{s_u} (M_n \bar{w}_{,n} + M_{ns} \bar{w}_{,s} - Q_n \bar{w}) ds \end{aligned} \quad (48)$$

3. Sandwich plate (with facing material thickness  $t_f \ll h$ ) with thermal strain effect

$$\begin{aligned} \pi_c = & \frac{1}{2} \int_A \frac{2}{E t_f h^2} \left[ (M_x + M_y)^2 + 2(1+\nu)(M_{xy}^2 - M_x M_y) + \frac{h^2 E t_f}{2 G h} (Q_x^2 + Q_y^2) \right] dA \\ & - \int_A \frac{2}{E t_f h^2} (1-\nu) M_o (M_x + M_y) dA \\ & - \int_{s_u} (M_n \bar{\phi}_n + M_{ns} \bar{\phi}_s - Q_n \bar{w}) ds \end{aligned} \quad (49)$$

where

$$M_o = \frac{E h t_f}{2(1+\nu)} \alpha (\Delta T_u - \Delta T_\ell)$$

The subscripts u and  $\ell$  indicate the upper and lower facing, respectively.

It can be seen that when Equations 45, 46, 48 or 49 are used in the formulation of the assumed stress finite element methods, an equation in the form of Equation 17 will result. Here the term  $\beta^T H_F \beta_F$  will arise not only from the particular solution for stresses but also from the terms involving  $M_{\alpha\beta p}$ ,  $Q_{\alpha p}$ ,  $M_{\alpha\beta} M_o \lambda_\theta$  and  $Q_\alpha Q_o \beta$ . Noting that the matrix  $H_F$  appears in the generalized nodal forces (see Equation 25) we can conclude that the initial strains will lead to equivalent nodal forces and the distributed load p will make further contribution to the generalized forces when the "moderately thick" plate theory is employed.

## SECTION IV

### BOUNDS TO DIRECT INFLUENCE COEFFICIENTS

Finite-element analyses by compatible and equilibrium models will yield bounds on the total strain energy content. Since the direct flexibility influence coefficient (i.e., the generalized displacement due to the corresponding generalized force of unit magnitude) is equal to the strain energy, its upper and lower bounds can also be established by the equilibrium and compatible models, respectively. This idea has been explored by Fraeijs de Veubeke (Reference 4)\* in dual finite element analyses of different types of structures.

The direct influence coefficient obtained by the finite element hybrid method may be either an upper or a lower bound, since the method is not based on a minimum principle. However, it can be shown that the direct influence coefficient by the hybrid model is always bounded by that of a compatible model using the same type of interelement boundary displacements and that of an equilibrium model using the same type of interior stresses.

We observe that within each element, the compatible model satisfies the compatibility conditions, while the hybrid model satisfies internal equilibrium. Therefore, a compatible model is more rigid than the hybrid model if the same set of generalized coordinates  $q$  and the same interpolating functions for the interelement boundary displacements are chosen. In that case, the direct influence coefficient obtained by the hybrid model will be larger than that obtained by the compatible model. For the compatible model, we can introduce additional displacement modes but keep the same set of generalized coordinates by the static condensation process (Reference 8). The introduction of such additional modes is to improve the satisfaction of the internal equilibrium. It is understood that the internal compatibility condition is always satisfied. On the other hand, the use of more and more stress modes  $\beta$  in the hybrid model improves the satisfaction of internal compatibility, while the internal equilibrium conditions are already satisfied. It is obvious that the two methods will yield exactly the same result if the assumed modes in both cases approach infinity. We can also interpret the use

of more displacement modes in the compatible model as a relaxation of artificial constraints. However, the use of more stress modes in the hybrid model would produce a structure more rigid than one with fewer stress modes.

For the equilibrium model, when a set of assumed stress modes is chosen, there is only one choice of generalized displacements. If the same stress modes are used in a hybrid model, the structure will be more rigid than the one analyzed by the corresponding equilibrium model because of the imposed compatibility conditions along the interelement boundaries. The direct influence coefficient of the hybrid method will be lower than that of the equilibrium method using the same stress modes. Table 1 gives a summary of the conditions fulfilled by the various finite element schemes. They are arranged according to increasing rigidity of the different models.

Since the finite element compatible model always yields a lower bound of the direct influence coefficient, it appears that the direct influence coefficient obtained by using more internal nodes is always superior to that obtained by using fewer or no internal nodes. No such conclusion can be made concerning the number of stress modes in the hybrid model. In fact, if the direct influence coefficient obtained by using  $i$  stress modes in that method is already a lower bound, then the use of  $j$  stress modes with  $j > i$  can only make the solution more inaccurate. Thus, there is an optimum number of assumed stress modes in the hybrid method.

There does not seem to exist any method that one can use to predetermine the optimum number of assumed modes. The situation will be different for different problems and for solutions at different locations of the structure. However, one can see immediately that the resulting error of the approximate solution may arise from both the error of the assumed stress field and that of the assumed boundary displacement. One can thus conclude that the two independent assumed functions should be comparable, i. e., that they should provide errors of the same order of magnitude. For example, in the plate-bending problem, if the assumed moment distribution in the interior of each element is a quadratic function of the space coordinates, the transverse shear distribution will be linear, then the order of magnitude of error of the boundary integral  $\int Q_n w ds$  will be comparable with that of  $\int M_n w_{,n} ds$  when  $w_{,n}$  is assumed to vary linearly along the boundary (Reference 3). The order of magnitude of the error cannot be reduced by including many assumed stress modes for the interior of an element without improving the boundary displacement function. Indeed, in the case of the hybrid model, the use of additional stress modes may actually decrease the accuracy of the solution. This argument of comparable errors in the assumed interpolating functions is

TABLE 1  
CONDITIONS SATISFIED BY VARIOUS FINITE-ELEMENT METHODS

Method	Symbol	Internal Equilibrium	Boundary Equilibrium	Internal Compatibility	Boundary Compatibility	Remarks
Equilibrium Model	e	YES	YES	NO	NO	Using the same stress modes
Hybrid Model Finite Number of Stress Modes	$h_m$	YES	NO	NO	YES	
Hybrid Model Infinite Number of Stress Modes	$h_\infty$	YES	NO	YES	YES	Using the same boundary interpolation function
Compatible Model Infinite Number of Displacement Modes	$C_\infty$					
Compatible Model Finite Number of Displacement Modes	$C_m$	NO	NO	YES	YES	

Direct Flexibility Influence Coefficients

$$(q/Q)_e > (q/Q)_{h_m} > (q/Q)_{h_\infty} = (q/Q)_{C_\infty} > (q/Q)_{C_m}$$



also applicable to the compatible model. The use of many additional internal modes for a given boundary displacement function again cannot reduce the order of magnitude of the error.

## SECTION V

### RESULTS OF FINITE-ELEMENT PLATE-BENDING ANALYSES

To illustrate the various points on the assumed stress methods brought up in this paper, several numerical results by finite-element methods are presented in this section.

1. The central deflection of a square plate with clamped edges under central loading has been analyzed by different finite-element methods using right-triangular elements. For comparison, the compatible model by Clough and Tocher (Reference 9), the equilibrium model by Fraeijs de Veubeke and Sander (Reference 10) and the hybrid model by Severn and Taylor (Reference 11) are discussed. The results are plotted in Figure 3 in terms of the percentage error versus the number of meshes in half of the plate width. The results clearly indicate the upper and the lower bound solutions, respectively, by the equilibrium and compatible models. It is seen that since in both the compatible model and the hybrid model the inter-element displacement functions are cubic in  $w$  and linear in  $w_{,n}$ , the latter model, according to our previous conjecture, yields a more flexible structure. On the other hand, since in the hybrid model the stress approximation involves quadratic terms in the moment while the equilibrium model relies on a less accurate linear distribution, the hybrid model leads to a comparatively more rigid structure. It should also be observed that the hybrid method provides a lower bound in this case and hence provides more accurate solutions than the corresponding compatible model.

2. The second example shown in Figures 4 and 5 is the central deflection of a simply-supported square plate under central load. Figure 4 shows the results obtained by using 12 degrees of freedom rectangular elements. However, in this case, an equilibrium model will result in an element with kinematical deformation modes. Hence, only the results of the

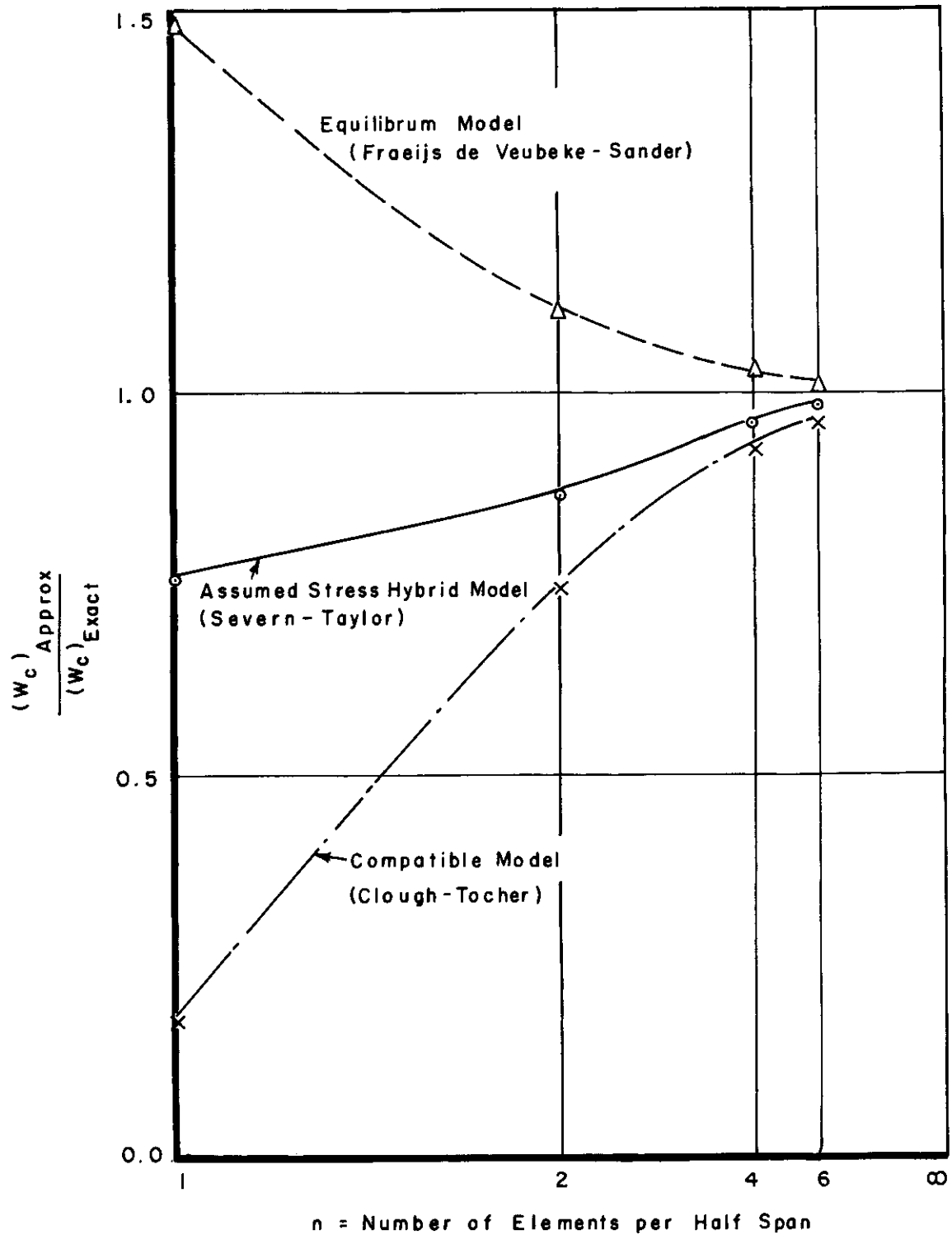


Figure 3. Center Deflection of Clamped Square Plate Under Center Load (Triangular Elements)

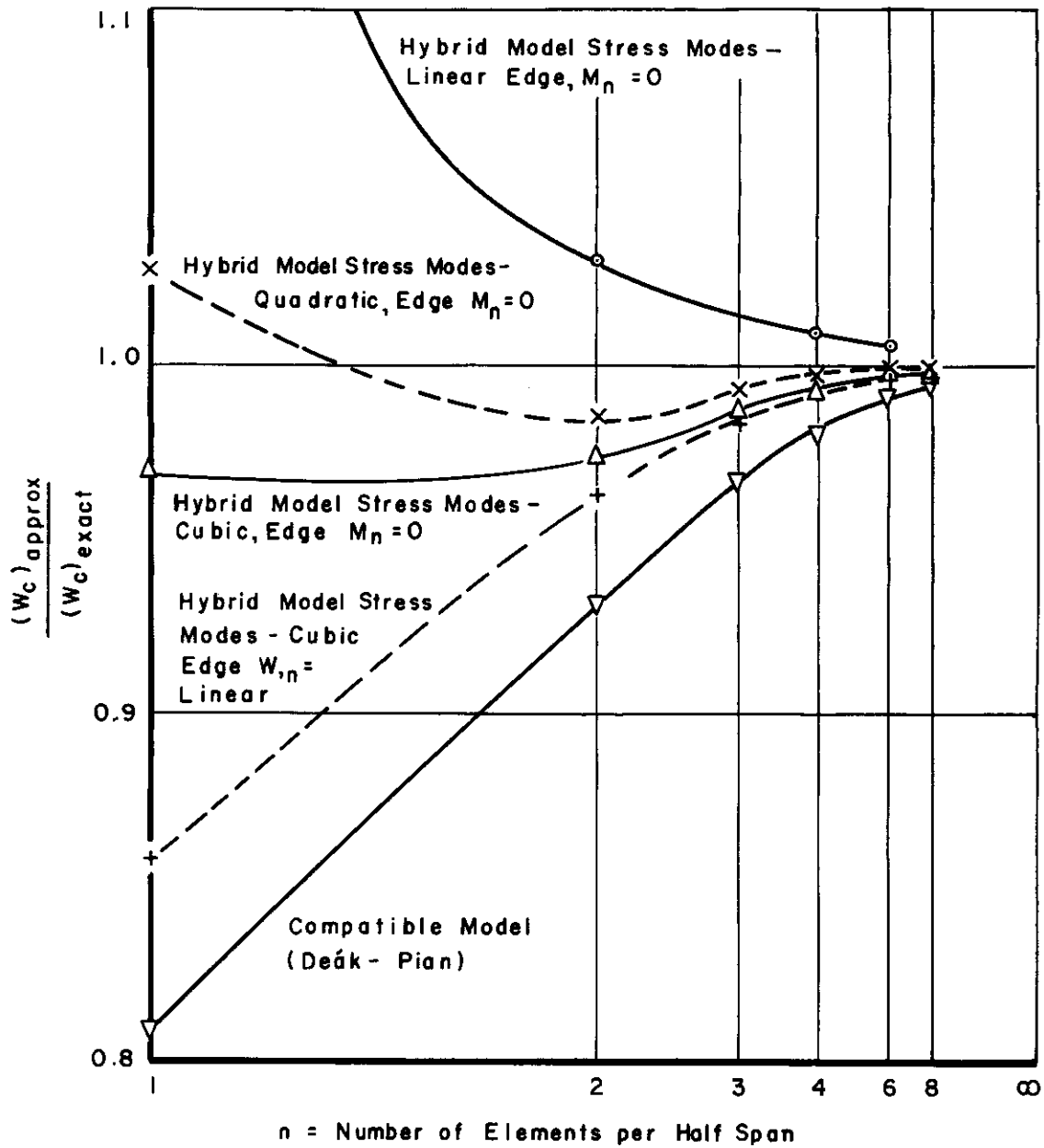


Figure 4. Center Deflection of Simply-Supported Square Plate Under Center Load (Rectangular Elements)

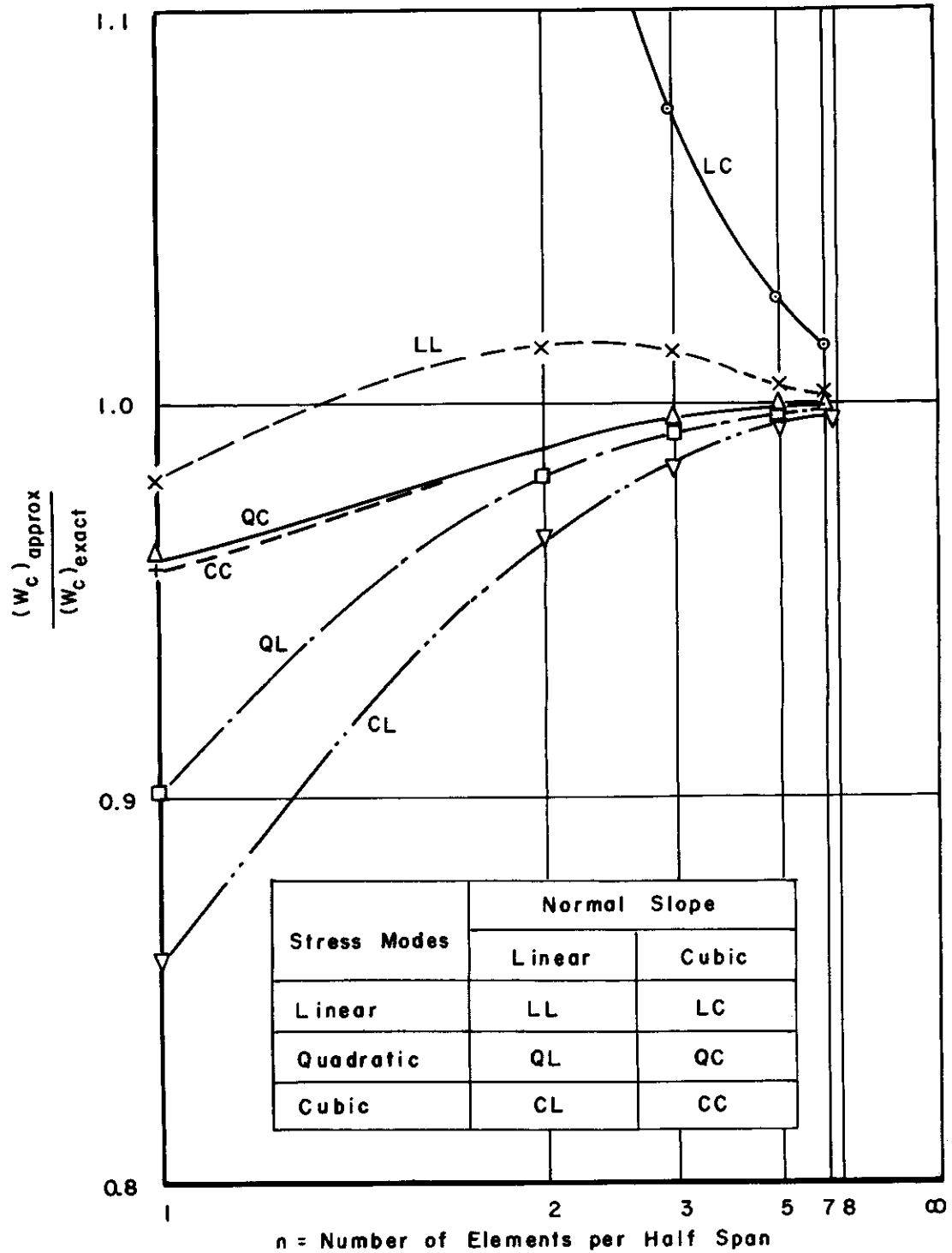


Figure 5. Center Deflection of Simply-Supported Square Plate Under Center Load (Assumed Stress Hybrid Method - Rectangular Elements)

compatible and hybrid models are presented for comparison. The formulation of the hybrid method for a rectangular plate element employed different moment approximations in the interior of each element. The assumed boundary displacements are cubic in  $w$  and linear in  $w_{,n}$ . The compatible model is the one used by Deák and Pian (Reference 12), hence involves the same boundary displacement approximation as the hybrid model.

It is clearly indicated here that the hybrid model may yield either the upper or the lower bound for the direct flexibility influence coefficient, and with the use of a sufficiently large number of stress modes, it will yield a lower bound solution. In the present case, the use of a quadratic moment distribution yields the most accurate results.

The hybrid solutions include two different approaches: in one case the assumed stress distribution satisfies the condition of vanishing normal moments  $M_n$  along the simply-supported edge; in the other, the prescribed boundary stress condition is not considered as a restrained condition. As indicated in the results, the first of these two approaches provides more accurate solutions, but the improvement becomes diminishingly small when a large number of elements is used in the analysis.

Figure 5 compares the results for the same problem obtained by using different combinations of interior stress approximations and boundary displacement approximations. In addition to the 12 degrees of freedom elements, the 16 degrees of freedom elements are used. For the latter, both  $w$  and  $w_{,n}$  vary as cubic functions along the edges. Also in these sets of solutions, the assumed stress modes do not satisfy the prescribed boundary condition of vanishing normal moment. This figure shows clearly that for most accurate solutions there is an appropriate combination of interior stresses and boundary displacements. For example, in this case, the linear-moment and linear-normal-slope combination appears to be a good choice. Then the use of more boundary displacement modes with the same linear moment distribution can only yield more inaccurate solutions corresponding to more flexible structures. In fact, as we have pointed out earlier, the over-abundance of the boundary displacement modes will cause the structure to be kinematically unstable. It is seen, however, that if the approximations for the interior stresses and boundary displacements are improved simultaneously, the accuracy of the solution can be improved.

3. The third example concerns a simply-supported square plate under uniform loading. For the hybrid model, a quadratic moment distribution is assumed, hence unique generalized nodal forces can be obtained. The center deflection of the plate has been calculated by such

a method using various mesh sizes as shown in Figure 6. It is seen that the convergence of the solution is extremely rapid in the uniform loading problem. Solutions have also been obtained by using inconsistent nodal forces which involve only vertical forces without moments. The results are much inferior to those obtained by using the consistently lumped nodal forces. Also included in the figure for comparison are the results by two compatible models using triangular elements obtained by Clough and Tocher (Reference 9) and by Bazeley, et al. (Reference 13), respectively, and by the equilibrium model obtained by Morley (Reference 14). In Morley's formulation, the unknown stress resultants (values of stress functions) are used as unknowns and the deflection of the plate can only be calculated by integrating the moment curvature relations. In view of the approximate character of the moments provided by the finite element analysis, the deflection obtained by integration is, in general, dependent upon the chosen integration path; hence is not a unique solution. Thus, two different solutions by Morley are shown in Figure 6.

Figure 7 is a comparison of the stress distributions ( $M_x$  along the axis of symmetry  $y = 0$ ) for this plate. It is seen that the assumed stress methods (equilibrium and hybrid models) can provide very accurate stress distributions while for the compatible model only stresses at the mid-points of the individual segments are reasonably close to the exact solutions.

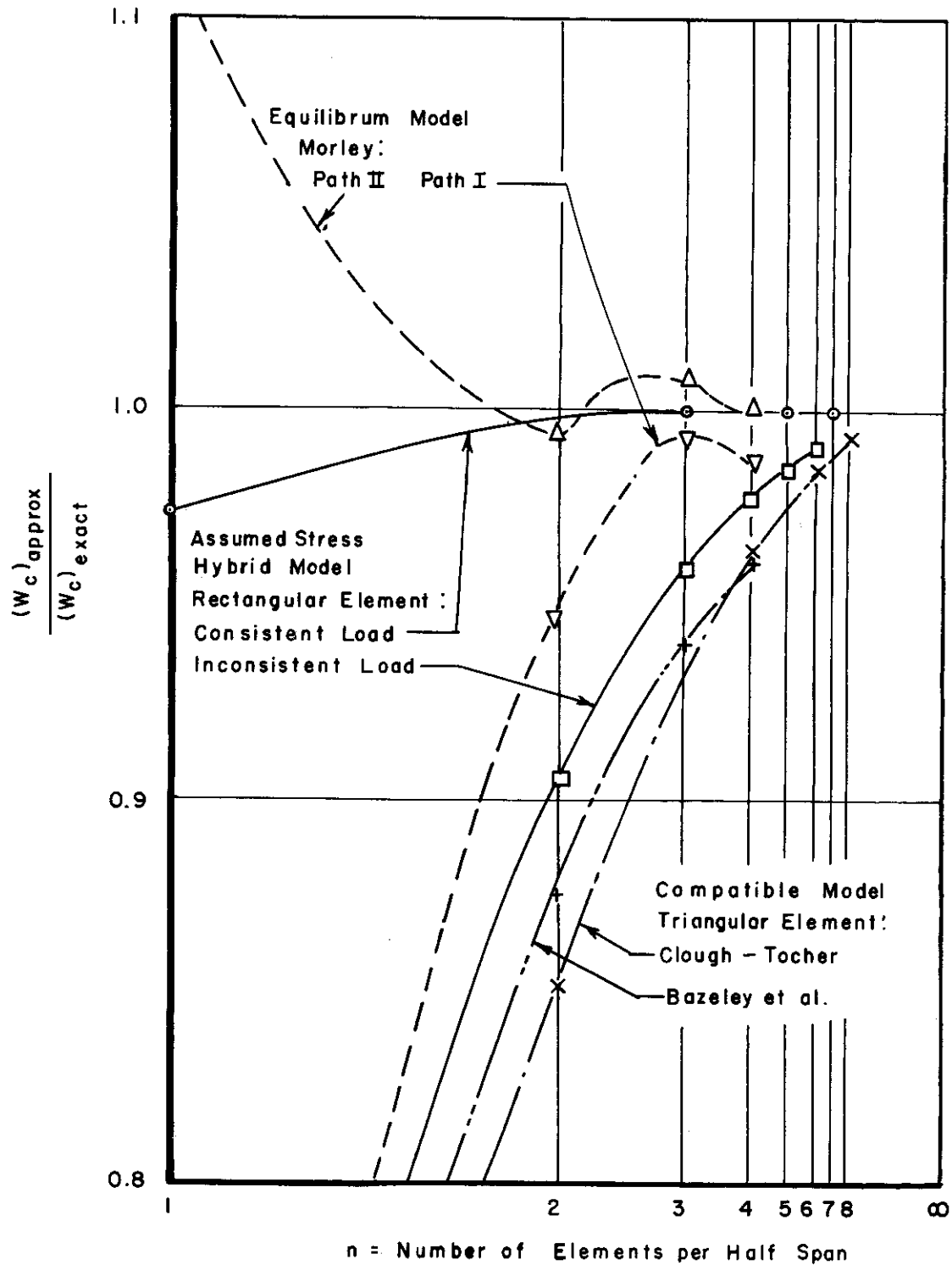


Figure 6. Center Deflection of Simply Supported Square Plate Under Uniform Loading

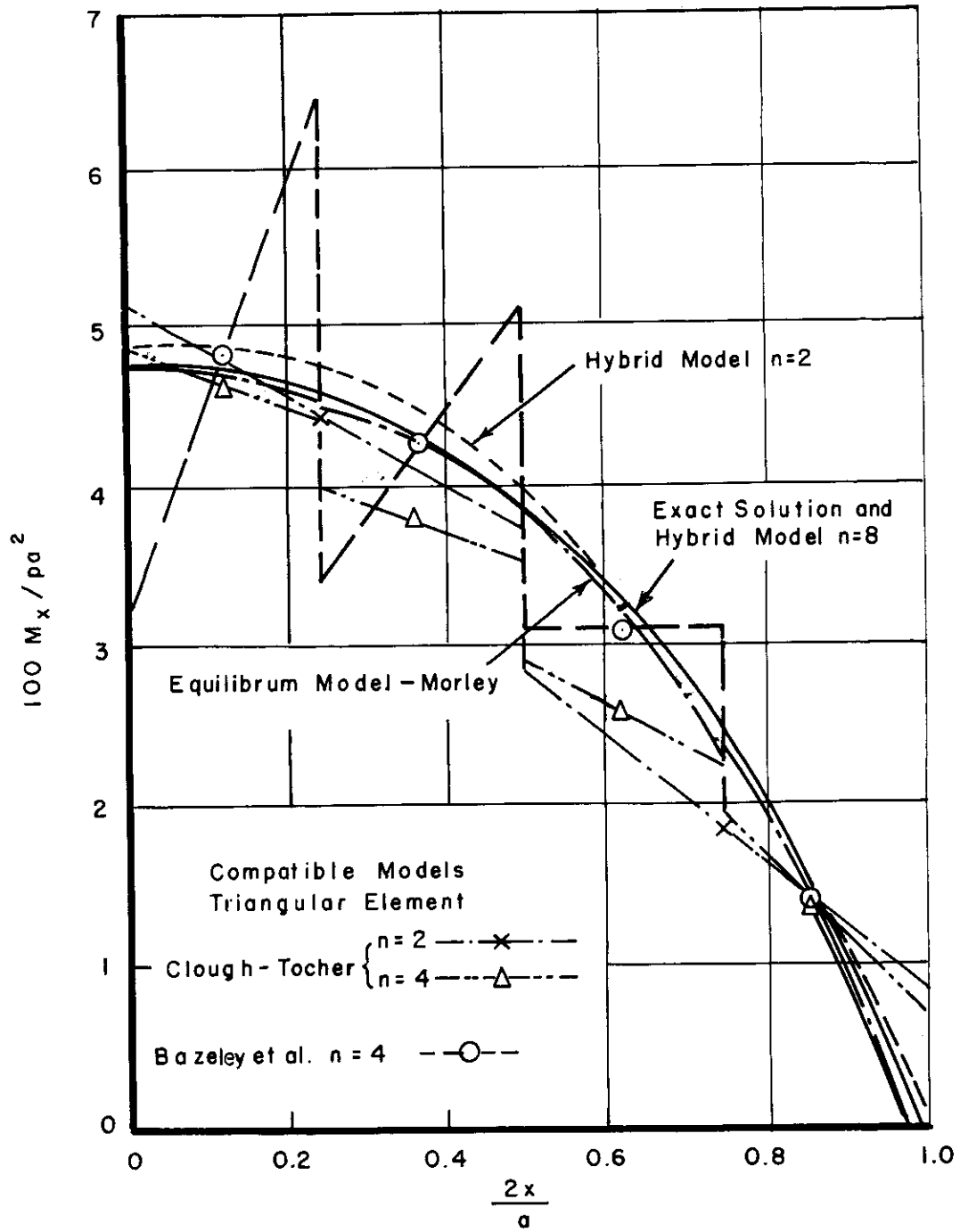


Figure 7. Bending Moment Along Center Line of Simply Supported Square Plate Under Uniform Loading



SECTION VI  
TRANSVERSE SHEAR EFFECTS IN PLATE BENDING

The inclusion of transverse shear effect in the plate-bending problems has received only limited attention in the finite element application. Herrmann (Reference 15) has included such effect in his formulation by the Reissner's principle. Severn and Taylor (Reference 11) have pointed out the convenience of taking transverse shear effect into account by the assumed stress hybrid model. Lundgren (Reference 16) has solved the problem of buckling of sandwich plates, the stiffness matrices of which are obtained by the assumed stress hybrid model.

Only until very recently was the "moderately thick" plate-bending problem solved by the finite-element method using compatible displacement functions (Reference 17). In that analysis Smith used the plate theory advanced by Love so that he can express the strain energy in terms of only  $w$  and the derivatives of  $w$ . However, he has to use 12 degrees of freedom at each node in his rectangular elements in order to account for the higher order derivatives of  $w$  in the strain energy functional. An alternative assumed-displacement approach for the "moderately thick" plate is to distinguish the rotations  $\theta_x$  and  $\theta_y$  from the derivatives  $w_{,x}$  and  $w_{,y}$ , respectively, and use five generalized coordinates at each node. If, in such a case, only  $w$ ,  $\theta_x$  and  $\theta_y$  are used as generalized coordinates at the nodes, the displacement functions  $w$ ,  $\theta_x$  and  $\theta_y$  can only be assumed linear along the boundary in order to maintain the compatibility and if the simplest interpolation functions (linear function for a triangular element and bilinear function for a rectangular element) are used, the strain representation will be extremely crude. In fact, it can be shown that by such a formulation, the shear strain energy will be predominating unless the element size is kept as small as the plate thickness. Thus a finite-element method formulated in this manner will, in general, yield very erroneous results. To improve the situation, the displacement functions must be much more complicated; hence many internal nodes are needed.

When the assumed stress hybrid model is used, the transverse shear effect can be taken into account accurately by including an adequate number of stress modes and the use of only  $w$ ,  $\theta_x$  and  $\theta_y$  as generalized coordinates can yield very reasonable solutions. Figure 8 indicates the results of a finite-element solution for the center deflection of a uniformly-loaded sandwich plate with the parameter  $\frac{a^2 G h}{\pi^2 D} = 4$ , where  $G$  = shear modulus of the core,  $h$  = thickness of the core and  $D$  = flexure modulus of the plate =  $E t_f h^2 / 2(1 - \nu^2)$ . In this assumed

stress hybrid formulation, the moment distributions are assumed quadratic while the boundary displacement  $w$ ,  $\theta_x$  and  $\theta_y$  are all linear. It is seen that by increasing the number of elements the solution converges very rapidly to the exact solution (Reference 18).

In the formulation of plate-bending with transverse shear effect by Severn and Taylor (Reference 11) and by Lundgren (Reference 16), the nodal displacements were still chosen as  $w$ ,  $w_x$  and  $w_y$  with  $w$  varying cubically and  $w_n$ , linearly along each edge. The correct choice should be  $w$ ,  $\theta_x$ , and  $\theta_y$  where  $\theta_x$  and  $\theta_y$  should be independent of  $w$ . Solutions obtained by using  $w$ ,  $w_x$  and  $w_y$  as generalized coordinates are also plotted in Figure 8. It is seen although such a solution is acceptable for large element sizes it becomes progressively inaccurate when the element size is reduced.

## SECTION VII

### CONCLUSIONS

The following conclusions can be drawn for the assumed stress hybrid method in the finite-element analysis:

- (1) The method is based on a rigorous variational principle.
- (2) This method yields a structure more flexible than that of a compatible model, but more rigid than that of an equilibrium model, in general.
- (3) A rational way has been obtained for consistent lumping of body and boundary forces.
- (4) To improve an element stiffness matrix, the approximations of both the interior stress distribution and boundary displacement distribution should be simultaneously and compatibly improved.
- (5) The method is particularly suitable to treat plate and shell problems taking transverse shear into account.

#### Acknowledgment

The authors acknowledge the assistance of C. H. Luk in carrying out the calculations.

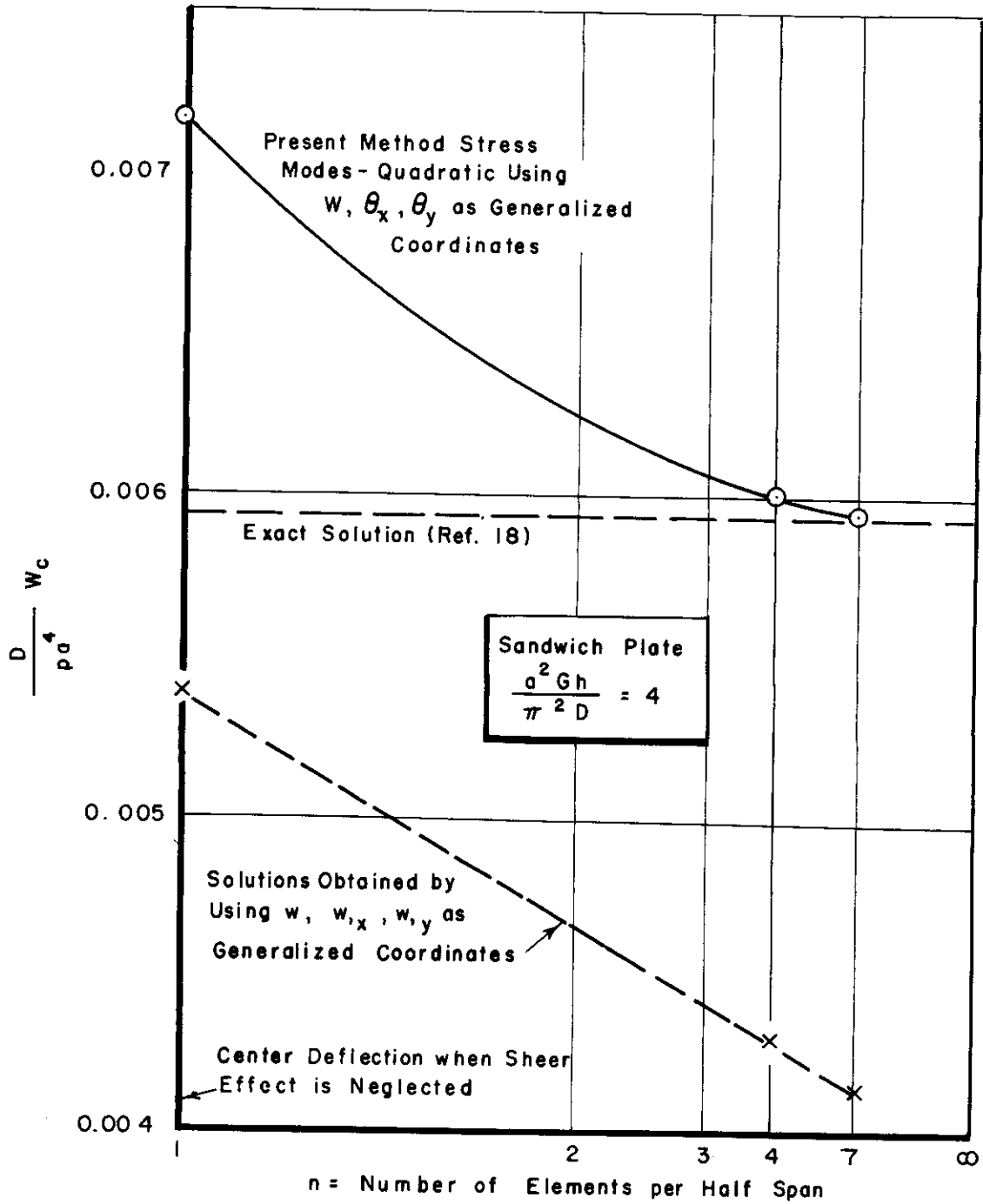


Figure 8. Center Deflection of Simply-Supported Square Sandwich Plate Under Uniform Loading

## SECTION VIII

## REFERENCES

1. Pian, T. H. H. "Derivation of Element Stiffness Matrices by Assumed Stress Distributions." AIAA J. 2, pp 1333-1336, 1964.
2. Pian, T. H. H. "Element Stiffness Matrices for Boundary Compatibility and for Prescribed Boundary Stress." Proc. of Conf. on Matrix Methods in Structural Mechanics. AFFDL TR-66-80, pp 457-477 (1965).
3. Tong, P., and Pian, T. H. H. A Variational Principle and the Convergence of a Finite-Element Method Based on Assumed Stress Distribution. AFOSR TR 68-0384, M.I.T. ASRL TR 144-1, Jan. 1968. (to be published in Intern. J. of Solids and Structures)
4. Fraeijs de Veubeke, B. "Upper and Lower Bounds in Matrix Structural Analysis." AGARDograph 72, pp 165-201, Pergamon Press, London (1964).
5. Fraeijs de Veubeke, B. "Displacement and Equilibrium Models in the Finite Element Method," Chapter 9, Stress Analysis, edited by O. C. Zienkiewicz and G. S. Holister, John Wiley and Sons (1965).
6. Washizu, K. Variational Methods in Elasticity and Plasticity. Pergamon Press, London (1968).
7. Reissner, Eric. "The Effect of Transverse Shear Deformation on the Bending of Elastic Plates." J. of Applied Mech. Vol. 12, p A-69 (1945).
8. Pian, T. H. H. "Derivation of Element Stiffness Matrices." AIAA J. 2, pp 576-577, 1964.
9. Clough, R. W. and Tocher, J. L. "Finite Element Stiffness Matrices for Analysis of Plate Bending." Proc. of Conf. on Matrix Methods in Structural Mechanics. AFFDL TR 66-80, pp 515-546, (1965).
10. Fraeijs de Veubeke, B. and Sander, G. "An Equilibrium Model for Plate Bending." Int. J. Solid Structures, Vol. 4, No. 4, pp 447-468, April 1968.
11. Severn, R. T. and Taylor, P. R. "The Finite Element Method for Flexure of Slabs when Stress Distributions are Assumed." Proc. Instn. Civil Engrs, 34 (1966), pp 153-170.
12. Deak, A. L. and Pian, T. H. H. "Application of the Smooth-Surface Interpolation to the Finite-Element Analysis." AIAA J. 5, No. 1, 1967, pp 187-189.
13. Bazeley, G. P., Cheung, Y. K., Irons, S. M. and Zienkiewicz, O. C. "Triangular Elements in Plate Bending - Conforming and Nonconforming Solution." Proc. of Conf. on Matrix Methods in Structural Mechanics, AFFDL TR 66-80, pp 547-576 (1965).
14. Morley, L. S. D. "The Triangular Equilibrium Element in the Solution of Plate Bending Problems." The Aeronautical Quarterly, Vol. 19, May 1968, pp 149-169.
15. Herrmann, L. R. "A Bending Analysis of Plates," Proceedings of Conf. on Matrix Methods in Structural Mechanics. AFFDL TR 66-80, pp 577-604 (1965).

REFERENCES (CONT)

16. Lundgren, H. R. "Buckling of Multilayer Plates by Finite Elements." Ph. D. Thesis, Oklahoma State Univ. May 1967.
17. Smith, I. M. "A Finite Element Analysis for 'Moderately Thick' Rectangular Plates in Bending." *Int. J. Mech. Sci.*, 10, pp 563-570, 1968.
18. Plantema, F. J. Sandwich Construction. John Wiley and Sons, 1966, p 71.

# *Contrails*